

## Kinetics of Assembly of a Parvovirus, Minute Virus of Mice, in Synchronized Rat Brain Cells

R. RICHARDS, P. LINSER, AND R. W. ARMENTROUT\*

Department of Biological Chemistry, University of Cincinnati College of Medicine, Cincinnati, Ohio 45267

Received for publication 7 January 1977

The rates of assembly of the three classes of particles of minute virus of mice were examined in synchronized rat brain cells by a combination of electron microscopy and biochemical techniques. We observed a burst of virus assembly beginning about 8 h after the end of cellular S phase. Labeled thymidine incorporated into the 1.46 g/cm<sup>3</sup> class of full virus particles was transferred almost quantitatively to the 1.42 g/cm<sup>3</sup> class. The 1.46 g/cm<sup>3</sup> virus appeared to be an immediate precursor to the 1.42 g/cm<sup>3</sup> class. Conversion of the 1.46 density virus to the 1.42 density particles was observed at the time of virus assembly. The processing was rapid and occurred primarily in the nucleus. Infected cells did not contain significant pools of viral DNA in a form that could be encapsulated in the absence of DNA synthesis. The role of the empty virus capsids in the assembly process is discussed.

Parvoviruses are the smallest known vertebrate DNA viruses (8). They are icosahedral particles 18 to 26 nm in diameter containing a single-stranded DNA molecule of  $1.5 \times 10^6$  to  $2.2 \times 10^6$  daltons (1). The parvoviruses can be divided into two groups, defective and nondefective, based on their ability to replicate with or without coinfection with adenovirus. Non-defective parvoviruses, including minute virus of mice (MVM), appear to be dependent on the S phase of the host cell for their replication (5, 9, 13). At least three distinct viral particles are produced in infected cells: empty capsids and two types of DNA-containing viral particles which can be separated in CsCl equilibrium density gradients (2, 3). No differences in the DNA content of the full particles have been observed (2, 14). However, the full virus particles each contain a different major capsid protein (B or C). There is a progressive loss of one full virus particle and accumulation of the other during the course of infection of randomly growing cells (2). Tattersall et al. have shown by tryptic peptide mapping that the capsid protein B may be converted to the capsid protein C by proteolytic cleavage (P. Tattersall, A. J. Shatkin, and D. W. Ward, *J. Mol. Biol.*, in press). In addition, Clinton and Hayashi have given evidence that infected cell extracts may convert precursor particle proteins to the product particle proteins in vitro (3). Although all of these observations are consistent with a precursor-product relationship between the two classes of full viral particles, the experiments have not excluded the possible independent

synthesis and differential turnover of the two particles in vivo. In addition, in previous experiments with randomly growing cultures, the product particle has been observed rather late in the course of infection, after the time required for a single round of viral replication. The possible late formation of this particle raised a question as to whether the putative processing event is a specific step in the assembly of the virus or a nonspecific degradation occurring in disintegrating cells.

In this report we have studied the synthesis and assembly of MVM in synchronized tissue culture cells using biochemical and electron microscopic techniques. We have also investigated the precursor-product relationship among the "full" viral particles, including the compartmentalization and transport of each density class.

### MATERIALS AND METHODS

**Virus isolation.** Plaque-purified MVM was the generous gift of Peter Tattersall. Virus was grown in RT-7 cells. The infected cells were detached from the surface of T flasks with 1 mM EDTA in phosphate-buffered saline (PBS) without calcium or magnesium, centrifuged, washed with PBS, and centrifuged. Cells were suspended in 0.01 M Tris, pH 9.0, and sonically disrupted. Cell debris was removed by low-speed centrifugation (1,500 rpm), and the virus preparation supernatant fluid was extracted with Freon twice. Magnesium chloride was added to 5 mM, DNase was added to 50 µg/ml, and the extract was incubated at 37°C for 1 h. The virus preparation was then layered on a 37-ml 15 to 30% sucrose gradient containing 5 mM EDTA-0.01

M Tris, pH 8. Gradients were centrifuged for 6 h at 25,000 rpm at 4°C in an SW 27 rotor. Full virus sedimenting at 110S was used for one-step synchronization infections. The 110S viral particles were further purified on CsCl density gradients with the use of a fixed-angle rotor head for maximal resolution. Cesium chloride gradients with an average density of 1.47 were centrifuged to equilibrium for 48 h at 35,000 rpm in a type 40 rotor. Lambda phage (1.503 g/ml), added to each gradient as a density marker, was titered on *Escherichia coli* N99 lambda-sensitive bacteria. Fractions from both sucrose and cesium chloride gradients were collected from the bottom of the tube. The density of the CsCl gradients was determined by refractive index and corrected by the lambda phage internal density marker. Hemagglutinin was measured by use of a 25- $\mu$ l sample plus 25  $\mu$ l of 5% mouse red blood cells in PBS. With this assay, the 1.46 g/cm<sup>3</sup> viral particles have a specific hemagglutination titer of 150 hemagglutination units/ $\mu$ g of protein; both the empty capsid and the 1.42 g/cm<sup>3</sup> virus particles have similar titers (470 to 479 hemagglutination units/ $\mu$ g protein).

**Cells and culture.** In an effort to optimize several parameters of viral growth in tissue culture, a number of established cell lines as well as secondary cultures of rodent cells were examined. We used the RT-7 line of rat brain tumor cells because of their superior viral yield, radiolabel uptake, and adaptability to synchronization by our methods. This line was isolated by William Au from a brain tumor induced in the offspring of a rat injected with ethyl nitrosourea during pregnancy. The RT-7 cells are pseudodiploid (Au and Soukup, unpublished data), grow rapidly as a monolayer, and have been passaged more than 40 times in culture. These cells were routinely maintained in antibiotic-free F-11 medium (MEM, GIBCO) supplemented with 5% heat-inactivated fetal calf serum (FCS, GIBCO). Cells were periodically checked for mycoplasma contamination and were mycoplasma-free by the criteria of autoradiography, orcein staining, and electron microscopy. For the purpose of viral infection or mitotic detachment synchronization, the cells were transferred to F-11 medium supplemented with 10% FCS, 100 U of penicillin/ml, and 100  $\mu$ g of streptomycin/ml (GIBCO).

**Synchronization.** Monolayers of RT-7 cells grown to 50% confluence in 150-cm<sup>2</sup> Corning T flasks in F-11 (GIBCO) with 5% heat-inactivated FCS were refed with fresh F-11 medium containing 10% FCS. After 24 h, the flasks were shaken vigorously to remove mitotic cells and loosely adhering cells. The monolayers were then refed with media prepared by mixing equal amounts of F-11 medium containing 10% FCS that had been preincubated with cells for 16 h plus fresh F-11 medium supplemented with 10% FCS (preconditioned medium). At 2 h after the initial detachment, the monolayers were shaken gently to remove mitotic cells. Detached mitotic cells from several T flasks were pooled, and samples for cell count and mitotic index determination were processed immediately. Samples of cells were then plated into either 75-cm<sup>2</sup> Falcon T flasks (for bio-

chemical analysis of virus production) or 25-cm<sup>2</sup> Falcon T flasks (for electron microscopy and as control samples for monitoring the degree of synchrony).

The degree of synchronization of the control cultures was monitored by the mitotic index and by determining the fraction of labeled nuclei by autoradiography. At intervals (see Results) during the experiment, 25-cm<sup>2</sup> T flasks were exposed to [*methyl-<sup>3</sup>H*]thymidine (1  $\mu$ Ci/ml) for 30 min. The monolayer was then washed with ice-cold PBS. The cells were swollen and lysed by exposure to 0.5% sodium citrate solution for 10 min at 37°C. The isolated nuclei were then pelleted at low speed and resuspended in ice-cold Carnoy fixative for 30 min. The sample was spread on a microscope slide and air-dried. The slides were washed extensively in 5% trichloroacetic acid followed by distilled water to remove excess label and were subsequently dipped in liquefied Kodak NTB2 nuclear track emulsion. After 1 week of exposure at 4°C, the slides were developed in Kodak D-19 chemical developer and stained with Giemsa. For each time point, more than 1,000 nuclei were scored for determinations of mitotoxic index and fraction of labeled nuclei.

**Infection.** At 3 h after the detachment of mitotic cells, purified filter-sterilized "full" virus (particles sedimenting at 110S in a sucrose gradient) ( $2 \times 10^6$  PFU/HA) diluted in F-11 medium was adsorbed for 1 h at 37°C. The amount of virus used (5 to 50 PFU/cell) was determined immediately prior to the experiments by titration of hemagglutinin in a 48-h infection of synchronized RT-7 cells. After virus absorption, monolayers were washed with F-11 medium and refed with preconditioned medium.

**Electron microscopy.** At 6, 12, 18, 20, 22, 24, 30, 38, and 48 h after mitotic detachment, infected and mock-infected control monolayers were washed and fixed with 4% glutaraldehyde in phosphate buffer for 60 min at 4°C. The monolayers were postfixed with 1% osmic acid in phosphate buffer, rapidly dehydrated in graded ethanol followed by hydroxypropyl methacrylate as the transition solvents, and flat-embedded in Luft epon. Beam capsules filled with the resin mixture were inverted onto the monolayer and separated from the culture flask after polymerization by immersion in liquid N<sub>2</sub>. Ultrathin sections of the monolayers were cut parallel to the plane of growth with a DuPont diamond knife and were mounted on 200-mesh copper grids. Staining was performed with a saturated solution of uranyl acetate in a mixture of equal parts of 70% ethanol and pure methanol for 30 min (11, 12), followed by lead citrate (7) for 15 min. Electron micrographs were taken on a Zeiss EM 9-A electron microscope at magnifications from 1,850 to 27,600.

**Isolation of nuclei.** Nuclei were isolated by the method of Wray (16). The medium was removed from monolayer cells grown in plastic T flasks, and the monolayer was rinsed with PBS. The cells were incubated in 5 ml of isolation buffer (0.5 M hexylene glycol, 1 mM CaCl<sub>2</sub>, 50  $\mu$ M piperazine-N,N'-bis[2-ethanesulfonic acid], pH 6.5) for 10 min at 37°C, removed from the T flask, and centrifuged at 1,500 rpm in a table-top centrifuge for 5 min. The cells were resuspended in 2 ml of isolation buffer and

lysed by passing through a 25-gauge needle. The nuclei were collected by centrifugation. The supernatant fluid was saved as the cytoplasmic fraction, and the nuclei were resuspended in 0.5 ml of isolation buffer. Phase-contrast microscopy showed greater than 95% of the nuclei free from cytoplasmic tags.

To determine the amount of nuclear DNA released into the cytoplasmic fraction, we labeled the cells for 30 min with [<sup>3</sup>H]thymidine and separated them into nuclear and cytoplasmic fractions. We found 4% or less of the trichloroacetic acid-insoluble tritium in the cytoplasmic fraction.

**Trichloroacetic acid precipitation and scintillation counting.** To each sucrose and CsCl gradient fraction sample, 25  $\mu$ l of FCS (GIBCO) was added as carrier followed by 2 volumes of cold 10% trichloroacetic acid. After incubation at 4°C for 1 h, samples were filtered through Whatman GFA filters and washed with 30 ml of 10% trichloroacetic acid and 5 ml of 95% ice-cold ethanol. Samples were solubilized with Soluene (Packard Instrument Co.) and counted in toluene-based scintillation solution.

**Gel electrophoresis.** Sodium dodecyl sulfate (SDS)-polyacrylamide gel electrophoresis was performed as described by Laemmli (6). Approximately  $5 \times 10^{10}$  to  $10 \times 10^{10}$  virus particles, as determined by optical density (14), were applied to each gel. The sample, in 0.05 M phosphate buffer, pH 7.5, was brought to 1% SDS, 1% 2-mercaptoethanol, and 0.01% bromophenol blue, boiled for 5 min, and layered onto a polyacrylamide gel containing 8.75% acrylamide and 0.233% bisacrylamide. After electrophoresis at 2.0 mA/gel for approximately 5 h, the gels were stained overnight with 0.25% Coomassie blue in methanol-water-acetic acid (5:5:1) at room temperature. The gels were destained at 37°C for 24 to 48 h in 15% methanol-7.5% acetic acid.

Gels were scanned at 550 nm on a Gilford scanning spectrophotometer to determine relative proportions of each stained protein by integration of the area under the absorbance peak. Approximate molecular weights were determined from standard proteins run in the same gel with the viral samples. The proteins employed as markers were rabbit phosphorylase A (92,500), ovalbumin (45,000), and iodinated bovine serum albumin (BSA, 68,000). These standards closely bracket the viral proteins in the gels. After electrophoresis and staining, each gel was split longitudinally, dried, and analyzed by autoradiography (Kodak X-ray film) to locate the iodinated BSA standard relative to the stained protein bands on the same gel. <sup>125</sup>I-labeled BSA was found to comigrate with unlabeled BSA.

## RESULTS

**Proteins of viral particles.** To examine the capsid proteins of the various viral particles, we extracted virus from infected, randomly growing RT-7 cultures several days after maximal levels of hemagglutinin had been produced. In sucrose gradients, the viral particles could be readily separated by sedimentation into two classes, the full virus (110S) and empty capsids

(70S) (1, 8). As shown in Fig. 1, [<sup>3</sup>H]thymidine was associated only with the 110S particles; the 70S particles did not contain detectable levels of DNA.

The proteins of the 70S and 110S particles were analyzed on SDS-acrylamide gels (Fig. 2). The empty capsid (70S) contained two proteins, an 85,000-dalton protein and a 68,000-dalton protein in the ratio, by weight, of 15:85, respectively (see Materials and Methods). These results are in accord with those obtained by Tattersall et al. (14). The 110S virus material isolated from sucrose gradients contained three proteins of 85,000, 68,000, and 65,000 daltons present in the ratio of 16:14:70, respectively (data not shown). When the 110S material was centrifuged to equilibrium in CsCl, two rather broad bands of virus were obtained with peak densities at 1.46 and 1.42 g/cm<sup>3</sup> (Fig. 3). In polyacrylamide gels, it could be seen that the 1.42 g/cm<sup>3</sup> virus particle contained the 85,000- and 65,000-dalton proteins in a ratio of 15:85, with a few very minor additional bands present. The virus of density 1.46 contained principally the 85,000- and 68,000-dalton proteins in the ratio 16:84. These molecular weights for the viral proteins in the 110S particles are consistent with those found by Tattersall et al. (14). In addition, our results confirm the observation of Clinton and Hayashi (2) that full MVM occurs as two separate density particles, each with a different major capsid protein. It should be noted that the 1.46 density viral particle was consistently observed, even in preparations harvested well after net virus synthesis had stopped.

To clarify the sequence of events in the assembly of MVM, it was necessary to analyze virus replication in a single-step infection of highly synchronized cells. Many of the methods

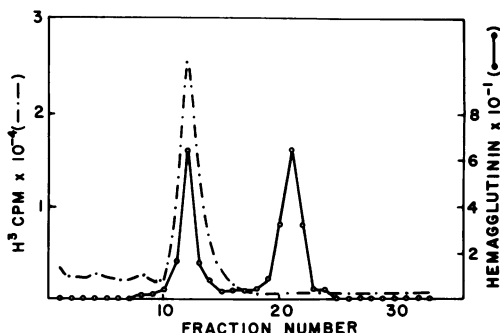
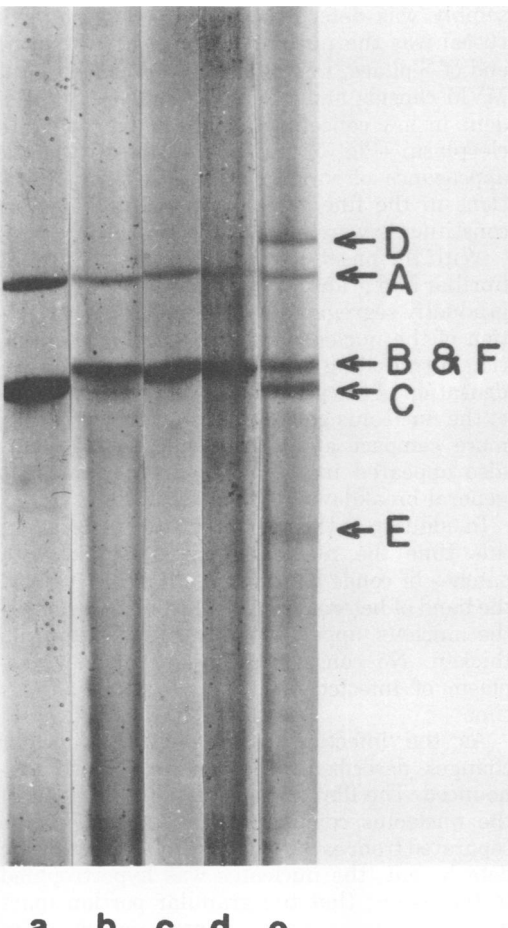


FIG. 1. Separation of full and empty minute virus of mice. Virus was grown in [<sup>3</sup>H]thymidine (5  $\mu$ Ci/ml) and purified on sucrose gradients as described in Materials and Methods. Fractions were collected from the bottom of the gradient.



**FIG. 2.** SDS-polyacrylamide gel electrophoresis performed on minute virus of mice particles. Virus particles were run in 8.75% gels at 2.0 mA/gel and were stained with Coomassie Blue: (a) 1.42 g/cm<sup>3</sup> and (b) 1.46 g/cm<sup>3</sup> isolated by CsCl equilibrium centrifugation; (c) empty virus purified by sucrose gradient centrifugation; (d) 1.46 g/cm<sup>3</sup> virus mixed with an equal amount of empty virus; (e) 1.42 g/cm<sup>3</sup> virus mixed with an equal amount of empty virus. The protein standards were run on the same gel, as described in Materials and Methods. (A, B, C) Viral proteins, (D) phosphorylase A (92,500), (E) ovalbumin (45,000), (F) <sup>125</sup>I-labeled BSA (68,000). Position indicated was determined by autoradiography of this gel after photography.

of cell synchronization, such as depriving cultures of essential nutrients or the use of inhibitors, are potentially disruptive to normal cellular processes. To avoid such complications, we synchronized RT-7 cells by manual detachment of mitotic cells in the absence of drugs. The degree of cell synchrony obtained by this

method is shown in Fig. 4. When initially detached, 25 to 35% of the cells were in metaphase and about 95% of the cells were in some stage of mitosis with varying degrees of chromosomal condensation observed. The length of S phase was 8 h, the G<sub>1</sub> phase was about 8 to 10 h, and G<sub>2</sub> was approximately 2 h. As measured by the fraction of labeled nuclei method, between a minimum of 75% and a maximum of 90% of the cells went through S phase together, and less than 1% of the cells were synthesizing DNA during the G<sub>1</sub> phase. The length of the cell cycle was approximately 20 h, as determined by the rise in the mitotic index.

**Kinetics of viral assembly.** The kinetics of virus assembly were examined both by electron microscopy and by biochemical analysis of synchronized infected RT-7 cultures. To closely correlate the two methods, we used samples for examination by electron microscopy that were taken from experiments in which biochemical techniques were used. Observations obtained by electron microscopy are presented first.

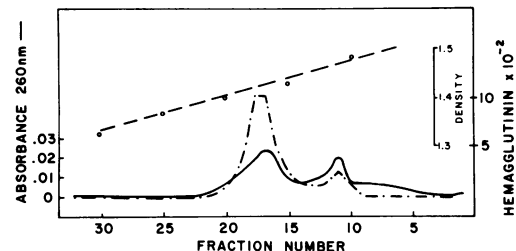


**FIG. 3.** CsCl equilibrium centrifugation of sucrose gradient-purified full minute virus of mice. The density determined by refractive index was corrected to the lambda phage ( $\rho$  1.50) density marker. Absorbance was measured on a Beckman 800 spectrophotometer as the gradient was pumped from the bottom of the tube through a 0.2-cm flow cell.

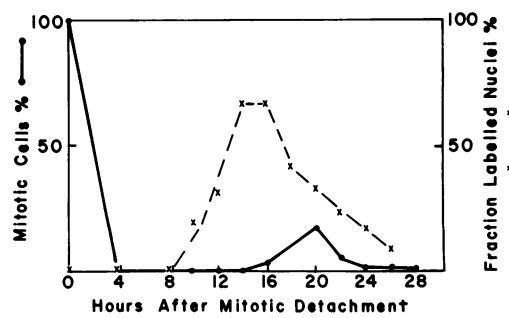


**FIG. 4.** Degree of synchronization of RT-7 cells. Mitotically detached cells were plated into 25-cm<sup>2</sup> T flasks and sampled for mitotic cells and fraction of labeled nuclei by autoradiography (as described in Materials and Methods).

**Mock-infected synchronized cells.** For purposes of comparison with infected cells, micrographs of typical interphase RT-7 cells synchronized and grown as described in Materials and Methods are presented in Fig. 5a and b. This particular cell was taken from the control sample at 24 h after mitotic detachment, when the bulk of the culture was in the G<sub>1</sub> phase.

The nuclei of control cells possessed the normal complement of fine filamentous euchromatin associated with clumps of presumed ribonucleoprotein (RNP) granules. An uneven thin band of condensed heterochromatin was evident lying at the periphery as well as in clumps throughout the nucleus. Three structural components were apparent in the nucleoli of these cells: light-staining fibrous material surrounded by tufts of dark-staining material (pars fibrosa, Fig. 5b), with granular RNP particles (pars granulosa, Fig. 5b) making up the remainder of the nucleolus. The three elements are arranged in a winding, skein-like manner which has been termed the nucleolonema (Fig. 5a and b).

The cytoplasm of control RT cells examined throughout interphase contained various concentrations of smooth and rough endoplasmic reticulum, often of the curvilinear variety. Mitochondria were numerous and normal in appearance. Numerous secondary lysosomes or heterophagosomes were observed in these cells, indicating that they were actively engaged in endocytosis (Fig. 5a).

**Electron microscope results—infected cells.** It has been shown for other parvovirus infections (5, 9) as well as for MVM (13) that growth of the virus is dependent on late S phase host cell cycle functions (see also below). Therefore, it is not surprising that little change in the normal ultrastructure of infected cells could be detected in the 6-, 12-, and 18-h (postmitotic harvest) samples. Figure 6 shows a section of cytoplasm in an infected cell at 18 h. The infected cells at this time are apparently as active biosynthetically as controls by virtue of the presence of high concentrations of rough endoplasmic reticulum, particularly of the curvilinear variety (Fig. 6). The only marked difference seen at this and earlier times during the infection between the infected and control cells was the presence in infected specimens of multivesicular bodies and apparent heterophagosomes containing MVM particles either as a lining on the inner membrane surface or as paracrystals (Fig. 6). Therefore, at least some of the input virus appeared to be taken up by the conventional methods for internalization of particulates.

The first location in which viral capsid as-

sembly was detected (as with other parvoviruses) was the nucleus (12). Shortly after the end of S phase, i.e., 20 h after mitotic harvest, MVM capsids and virus particles became evident in low concentration throughout the nucleoplasm (Fig. 5c and d). Accompanying the appearance of viral particles, several alterations in the fine structure of normal nuclear constituents were apparent.

With the onset of viral capsid assembly, the fibrillar and granular elements of the nucleolus gradually segregated with a centrifugal migration of the nucleolonema to a peripheral position surrounding the nucleolus (Fig. 5d). Condensation of the granular and fibrous elements of the nucleolus gave the nucleolus a generally more compact and dense appearance. Clefts also appeared in the nucleolus, indicating a general breakdown of its integrity.

In addition to the changes in the nucleolus at this time the nucleus became spotted with patches of condensed chromatin (Fig. 5c), and the band of heterochromatin at the periphery of the nucleus appeared denser and began to thicken. No consistent changes in the cytoplasm of infected cells were evident at this time.

As the infection progressed, the nuclear changes described above became more pronounced. The fibrous and granular elements of the nucleolus condensed further and became separated from each other. By 24 h after mitotic detachment, the nucleolus was hypertrophied to the extent that the granular portion (pars granulosa) was condensed into compact, often spherical structures sometimes associated with remnants of condensed fibrous material (Fig. 7a). Condensed material reminiscent of the dark and light fibrous elements of the nucleolus could be seen to take up diverse positions throughout the nucleus (Fig. 7a). Further condensation of euchromatin was also evident, causing an increase in size of the marginated band of heterochromatin, as well as the scattered tufts of condensed chromatin.

Clusters of pleiomorphic granules associated with fibrous material as described by Singer and Toolan in H-1 infection (11, 12) also appeared scattered throughout the nucleus at this time (i.e., 24 h after mitotic detachment; Fig. 7a, b, and c). These "clusters" of material had no apparent specific relationship with any other structure in the nucleus, as they could be seen associated with nucleolar vestiges or patches of condensed chromatin, or autonomously scattered throughout the nucleus. These "clusters" may represent, as suggested by Singer and Toolan (11, 12), RNP particles displaced from euchromatin by viral proteins.

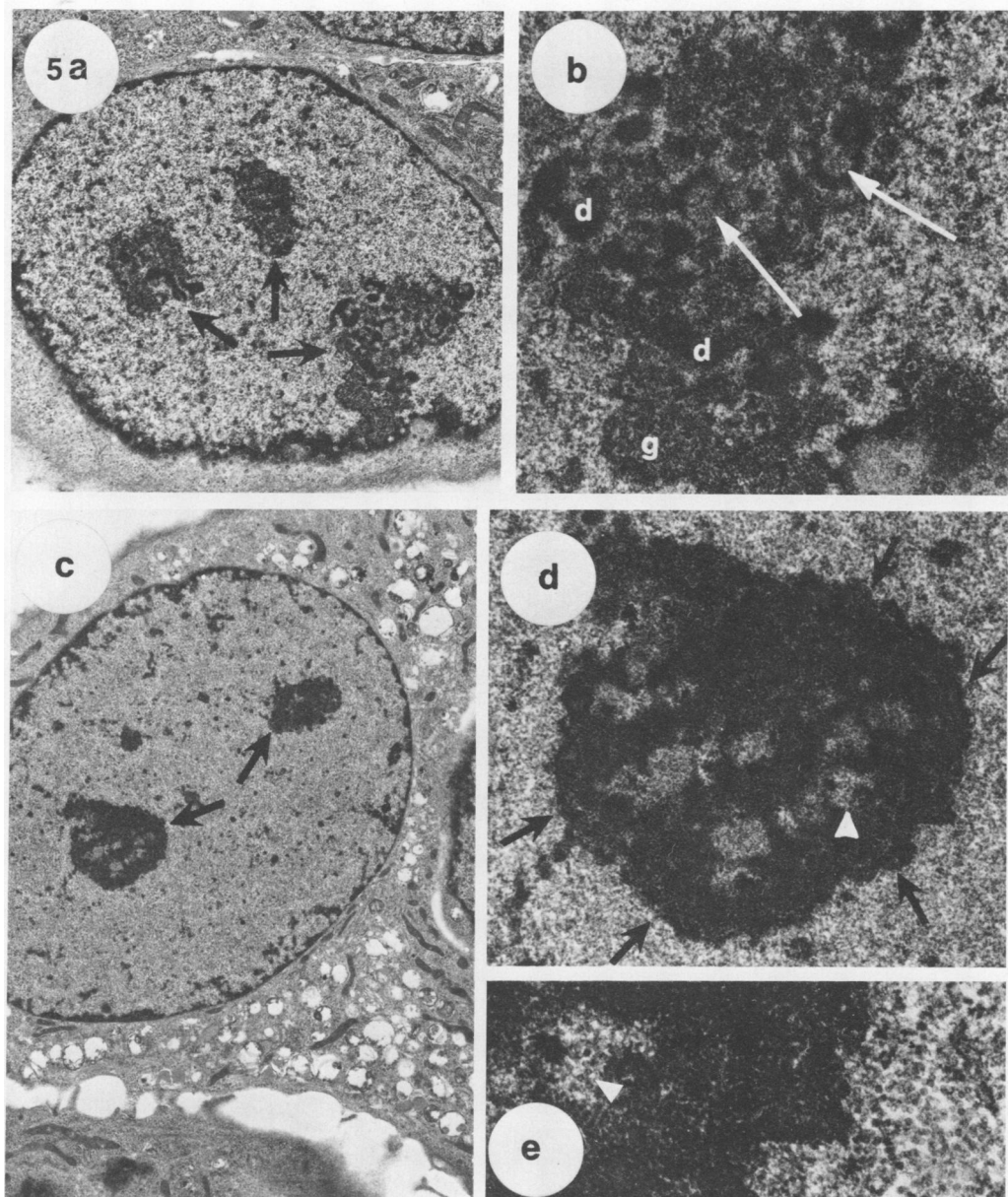


**FIG. 5.** (a) Control interphase RT cell 24 h after mitotic detachment. Note the appearance of normal nucleoli (arrows).  $\times 5,500$ . (b) Higher magnification of nucleolus shown in 5a. Note light (white arrows) and dark (d) fibrous elements (pars fibrosa), granular element (g) (pars granulosa), and the skein-like nucleolonemal substructure of the nucleolus.  $\times 19,350$ . (c) Infected RT cell 20 h after mitotic detachment. Nucleus is somewhat enlarged in comparison to control (Fig. 5a; note difference in magnification between control and infected), and the nucleoli (arrows) have begun to change in appearance.  $\times 4,000$ . (d) Higher magnification of degenerating nucleolus in Fig. 5c. Nucleolonemal substructure has undergone a centrifugal migration, forming a peripheral band surrounding the nucleolus (arrows). Numerous viral capsids are evident in the nucleoplasm as well as in clefts which have formed in the nucleolus (white arrowhead). The relationship between fibrillar and granular elements of the nucleolus has disappeared, and the entire structure has condensed somewhat.  $\times 19,350$ . (e) Blow up of lower right-hand section of Fig. 5d showing viral capsids in cleft in nucleolus (white arrowhead) as well as in surrounding nucleoplasm.  $\times 40,600$ .

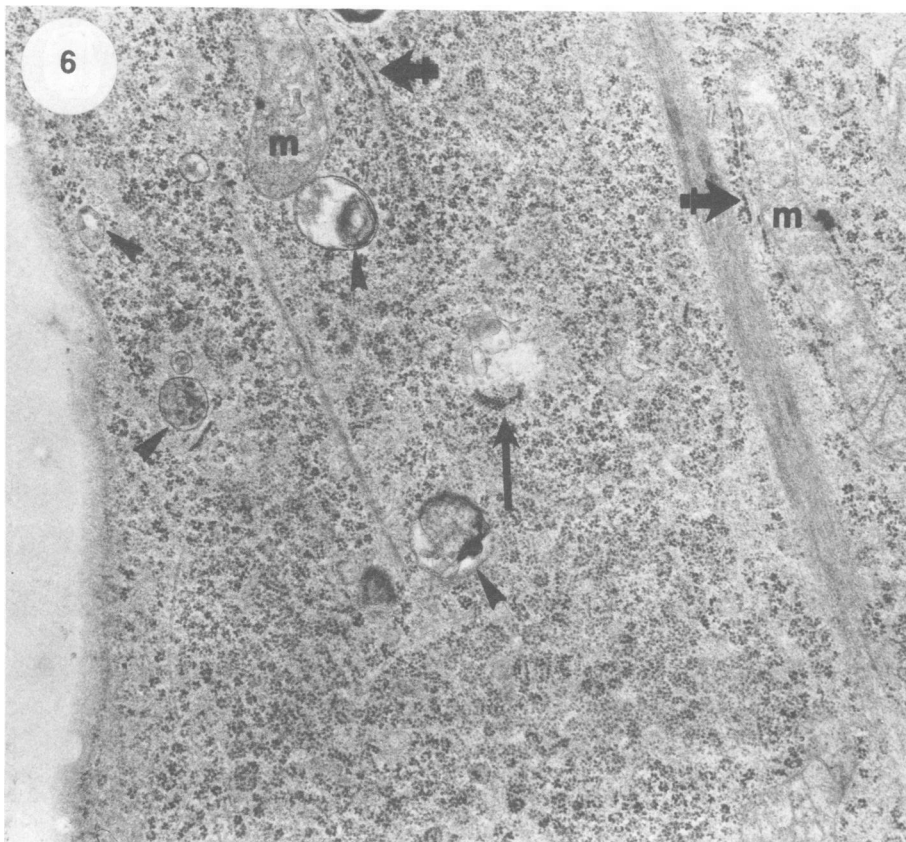


FIG. 6. Infected synchronized RT cell 18 h after mitotic detachment. Section through cytoplasm showing minute virus of mice paracrystal within multivesicular body (arrow), other presumed heterophagosomes (arrow heads), mitochondria (M), rough endoplasmic reticulum (crossed arrows), and high concentration of curvilinear polysomes throughout.  $\times 21,500$ .

Again, there was little if any change in cytoplasmic constituents by this stage of the infection.

The general picture for infected cells at 24 h after mitotic detachment remained somewhat the same through the next 6-h period, which encompassed the time of peak viral encapsulation (see below). Remnants of the granular elements of the nucleolus became less abundant, and the regions of densely compacted chromatin began to have irregular holes reflecting further degeneration. The cytoplasm of the cells by 30 h after mitotic detachment showed an increasing concentration of particles that appeared to be free ribosomes, with a concomitant decrease in the concentration of rough endoplasmic reticulum.

By 38 h after mitotic detachment, the infectious cycle had apparently passed its climax and some of the cells had begun to lyse. The intranuclear concentration of virus particles and capsids had dropped dramatically. The

dense band of marginated heterochromatin had expanded and dispersed somewhat, giving it a more granular and less compact appearance. Tufts of loosely knit fibrous material as well as extremely dense spheres of amorphous material remained among the now sparse population of viral capsids (Fig. 8a). On the rarefied background, fibrous material with viral capsids aligned along these fibers could be seen (Fig. 8b). The perinuclear space became distended at this time and was seen to contain a light amorphous matrix. General degeneration of the cytoplasm occurred at this time, and little of the cytoplasmic constituents remained (Fig. 8a).

The appearance of the infected RT cell nucleus differed to some extent, depending upon the conditions of infection. The cells in Fig. 5 through 8 from synchronized cultures were infected at high multiplicity (see Materials and Methods). In ultrathin sections, the most easily identifiable virus particle was the empty capsid, which appeared to be present in excess

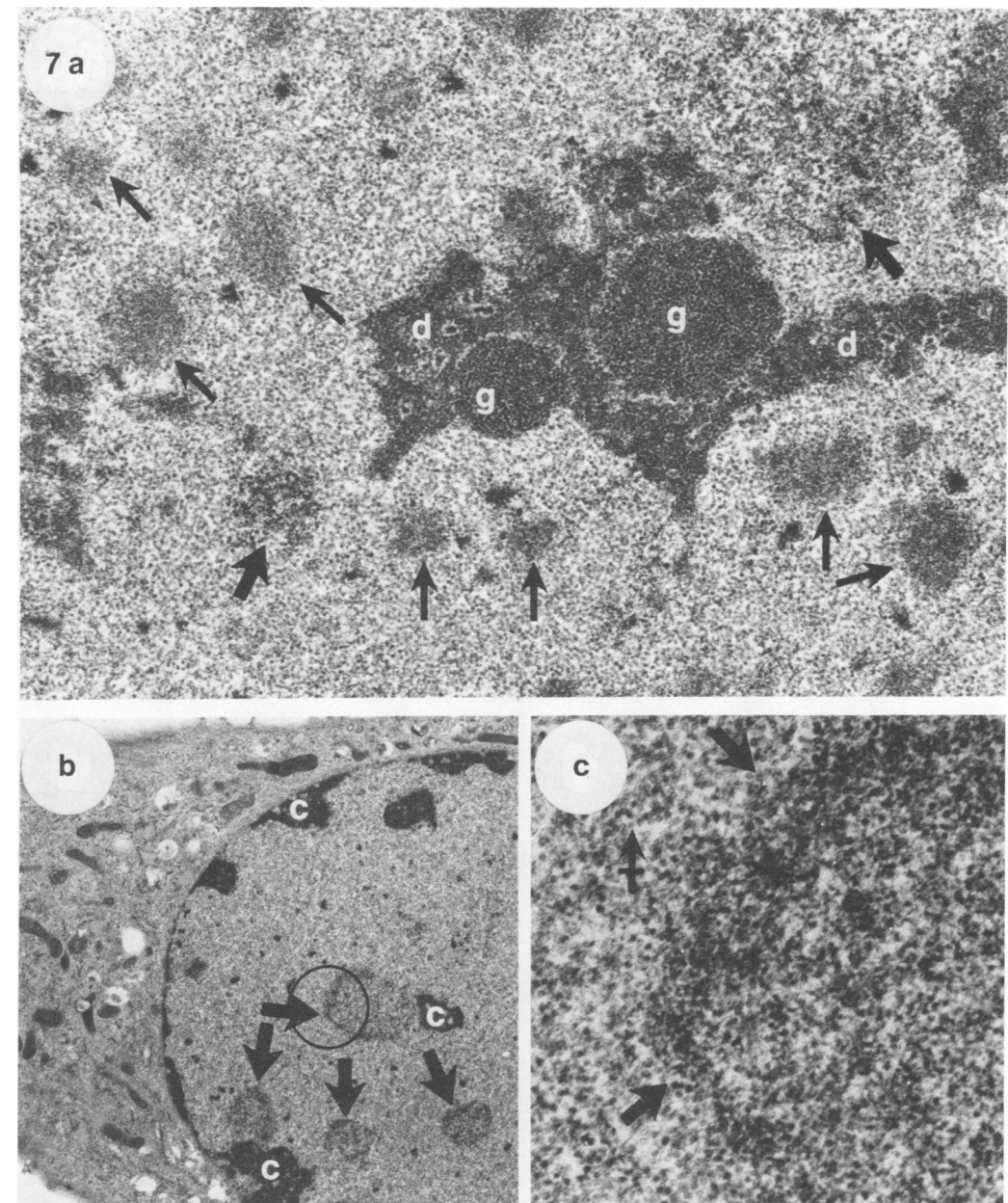


FIG. 7. (a) Area of an infected RT cell nucleus 24 h after mitotic detachment. The nucleoplasm is heavily congested with viral capsids, and the nucleolus has broken down into its component parts. The pars granulosa has condensed into spherical structures (g), and the presumed light (small arrows) and dark (d) pars fibrosa have apparently separated. Clusters of pleiomorphic interchromatin granules (large arrows) also appear scattered throughout the nucleus.  $\times 25,100$ . (b) Infected RT cell 24 h after mitotic detachment. The nucleus is swollen with viral particles. Heavily condensed chromatin (c) lies at the periphery of the nucleus and in patches throughout. Clusters of pleiomorphic interchromatin granules are seen closely associated with condensed chromatin as well as autonomously.  $\times 5,300$ . (c) Enlargement of circled area in Fig. 7b showing viral capsids (crossed arrow) and pleiomorphic interchromatin granules (large arrows).  $\times 40,600$ .

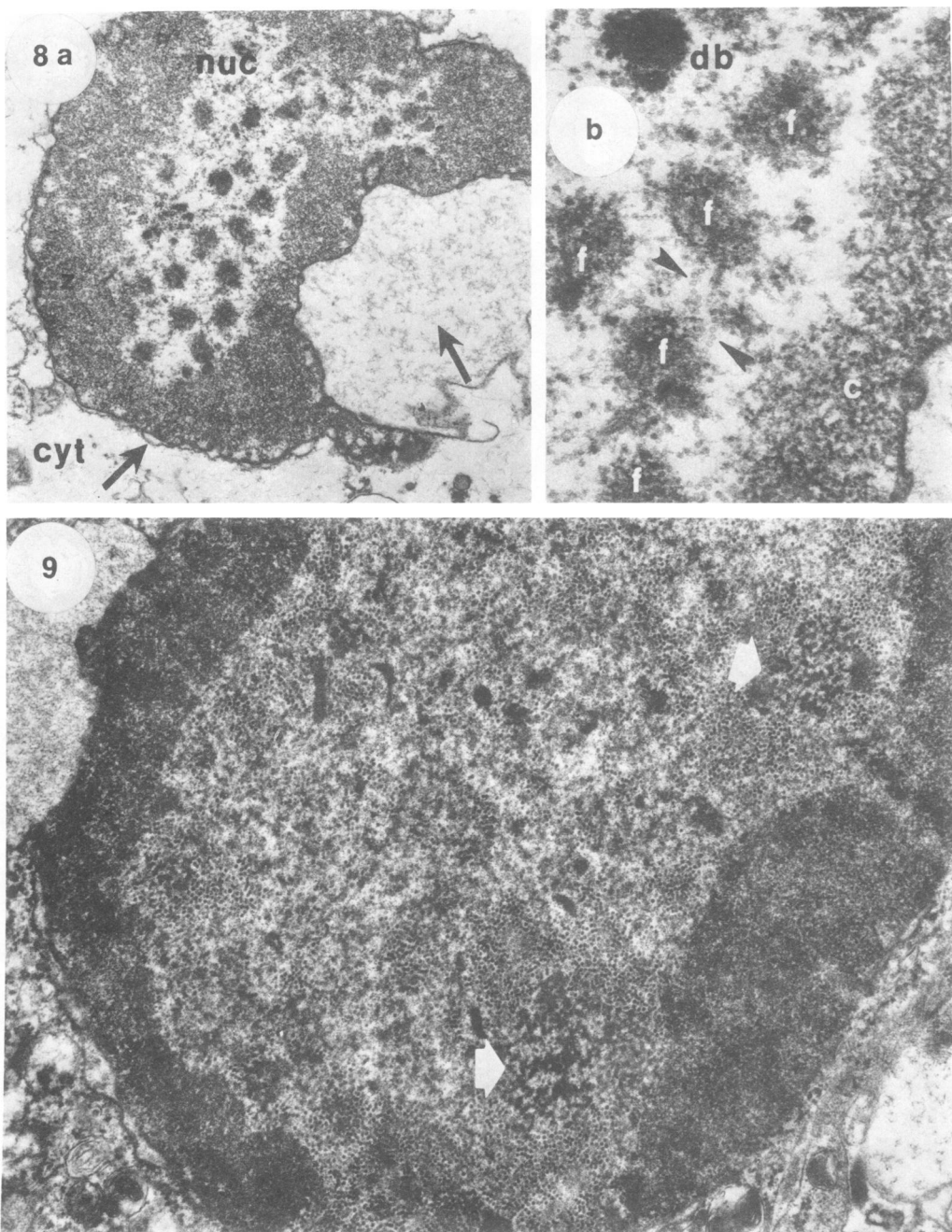


FIG. 8. (a) Infected RT cell 38 h after mitotic detachment. Degeneration of the cell is extensive, with rarefied cytoplasm (cyt) and nucleoplasm (nuc). The perinuclear space is distended (arrows), and the condensed chromatin at the periphery of the nucleus is somewhat more dispersed than at earlier stages of the infection.  $\times 12,900$ . (b) Enlargement of area of Fig. 8a showing dispersed band of chromatin (c), islets of residual fibrous material (f), a dense body (db), and linear arrays of viral capsids situated along fibrous material (arrow heads).  $\times 40,600$ .

FIG. 9. Randomly growing RT cell 12 h after a low-multiplicity infection. Note the relatively high proportion of full (dark staining) particles produced (compare to Fig. 5 and 7). The white arrows point out two skein-like structures closely associated with high concentrations of virus. These structures do not appear in the higher-multiplicity synchronized infection.  $\times 25,300$ .

relative to the full particle. Quantitation of the hemagglutinating activity produced in these cultures indicated that about six times more of the empty capsids were produced than the full particles (Fig. 10). However, when randomly growing RT cells were infected at much lower multiplicity (in this case 1,000-fold lower multiplicity), full virus was the predominant nuclear species produced during the first 12-h period (Fig. 9). Differences in the appearance of the infected nucleus were observed under these conditions, notably the existence of balls of ropelike material closely associated with high concentrations of full virus (Fig. 9). A detailed analysis of these observations will be published elsewhere.

**Biochemical results—rates of assembly of viral particles.** The rates of synthesis of virus particles were examined biochemically in the following manner. At 14, 20, 28, and 37 h after mitotic detachment, samples of the synchronized, infected cultures were exposed to [<sup>3</sup>H]thymidine (150  $\mu$ Ci/ml) for 3 h. The viral particles were then extracted from each sample, and the full virus was separated from empty capsids on sucrose gradients. The rate of synthesis of the full virus could be measured by the amount of [<sup>3</sup>H]thymidine label incorporated into the 110S region of these gradients. The total amount of virus accumulated was determined from the hemagglutination titers of the 110S (full virus) and 70S (empty capsid) regions.

As early as 17 h after mitotic detachment, slight amounts of both full and empty virus could be measured. However, it would appear by extrapolation that, although the rates of accumulation of the full and empty particles were similar, the empty capsid may begin to be synthesized slightly before the full virus (Fig. 10). Although increasing amounts of virus particles of both classes were detected in each subsequent time interval up to 72 h, there was a high rate of assembly of both full and empty particles in the interval of 28 to 31 h after cell synchronization. After this burst of viral assembly, viral synthesis continued, but at a very much diminished rate. These results support the observations obtained by electron microscopy; virus assembly began at 20 hr, peaked at about 28 h, and was virtually over by 38 h. In addition, the kinetics of viral assembly observed here demonstrate that the majority of susceptible cells in these cultures were producing virus synchronously.

The 110S viral material synthesized during the peak period of virus assembly (28 to 31 h postdetachment) was further analyzed on a CsCl gradient. Seventy-five percent of the

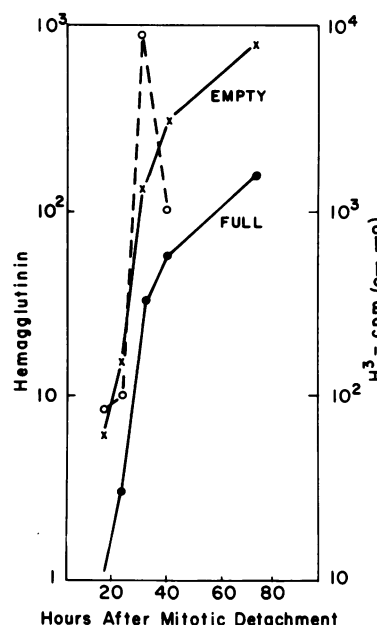


FIG. 10. Rates of virus assembly and accumulation in synchronized cells. RT-7 cells were mitotically detached and infected 3 h later. [<sup>3</sup>H]thymidine (150  $\mu$ Ci/ml) was added for 3 h at 14, 21, 28, and 37 h postdetachment. The labeled full virus was isolated from a sucrose gradient (○), and total full (●) and empty (x) virus was measured by hemagglutination. Note that both [<sup>3</sup>H]thymidine incorporation and hemagglutinin titers are presented on logarithmic scales.

[<sup>3</sup>H]thymidine-labeled virus was of the 1.46 density class and 25% was of the 1.42 density class (data not shown). The 1.42 density virus particles appeared during the period of maximal virus assembly, well before the infected cells had begun to seriously deteriorate, as ascertained by electron microscopy.

**Conversion of 1.46 density particles to 1.42 density MVM.** To determine whether the 1.46 density particle was processed to form the 1.42 density particle in vivo, we employed a "pulse-chase" experiment. Infected, synchronized RT-7 cultures were exposed to [<sup>3</sup>H]thymidine for 2 h during the period of the highest rate of virus assembly (28 to 30 h postdetachment). The synthesis of DNA was then inhibited with hydroxyurea, and excess unlabeled thymidine was added to the medium to dilute any labeled thymidine released to internal nucleotide pools by the breakdown of DNA.

**"Chase" conditions.** Preliminary experiments were undertaken to determine the minimal effective level of hydroxyurea and the effectiveness of our "chase" conditions. Uninfected,

unsynchronized RT-7 cells were labeled with [<sup>3</sup>H]thymidine (150  $\mu$ Ci/ml) for 2 h. The [<sup>3</sup>H]thymidine-labeled medium was removed, the cultures were rinsed with unlabeled medium, and preconditioned medium containing hydroxyurea (25  $\mu$ g/ml) and unlabeled thymidine was added to the cells. The concentration of unlabeled thymidine (2.5 mM) was 1,000 times that of the [<sup>3</sup>H]thymidine originally added. Figure 11 shows the effectiveness of this combined treatment in the inhibition of DNA synthesis. Under the "chase" conditions, net [<sup>3</sup>H]thymidine incorporation ceased within 20 min, and there was a linear decrease in alkali-stable, acid-precipitable label. We have consistently observed this loss of trichloroacetic acid-precipitable label on addition of hydroxyurea (5 to 50  $\mu$ g/ml) to cultures which have been labeled with [<sup>3</sup>H]thymidine for brief periods. It is likely that a significant amount of newly synthesized DNA breaks down when cells are exposed to hydroxyurea.

As shown in Fig. 12, we have determined the amount of residual DNA synthesis which occurs in the presence of hydroxyurea (25  $\mu$ g/ml) but in the absence of excess unlabeled thymi-

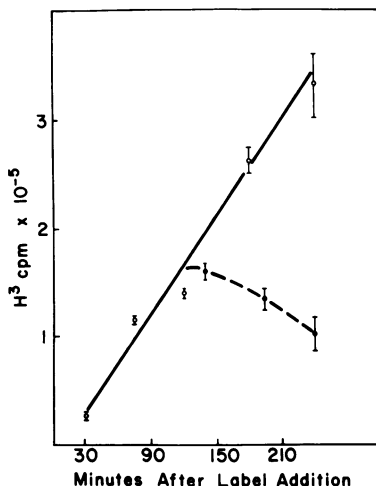


FIG. 11. Inhibition of DNA synthesis by hydroxyurea in the presence of unlabeled thymidine. Randomly growing RT-7 cells were labeled with [<sup>3</sup>H]thymidine (150  $\mu$ Ci/ml), and DNA synthesis was inhibited 2 h later by removal of [<sup>3</sup>H]thymidine and addition of hydroxyurea (25  $\mu$ g/ml) and unlabeled thymidine (2.5 mM). Cells were lysed in 0.1 N NaOH, and incorporation of [<sup>3</sup>H]thymidine was determined by trichloroacetic acid precipitation of the lysates. Samples were taken in triplicate, with the error bars representing the standard error of the mean for each time point. Symbols: ●, culture treated with hydroxyurea and thymidine; ○, control culture.

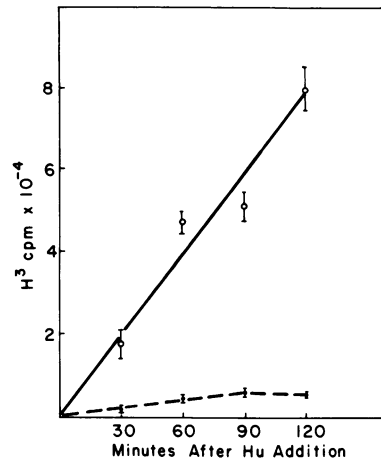


FIG. 12. Residual DNA synthesis in hydroxyurea (*Hu*)-treated cells. Hydroxyurea (25  $\mu$ g/ml) was added to randomly growing RT-7 cells, and [<sup>3</sup>H]thymidine (150  $\mu$ Ci/ml) was added 10 min later (●). Control samples contained no hydroxyurea (○). Samples were processed for incorporation of [<sup>3</sup>H]thymidine as described in the legend to Fig. 11. Samples were taken in triplicate, with the error bars representing the standard error of the mean for each time point.

dine. At 10 min after the addition of hydroxyurea to unsynchronized RT-7 cultures, [<sup>3</sup>H]-thymidine was added, and incorporation of label was measured at 30, 60, 90, and 120 min. At 60 min after the addition of [<sup>3</sup>H]thymidine, the amount of incorporated label found in the hydroxyurea-inhibited cultures was only 10% of that observed in normal control cells. From 60 to 120 min, no further label was incorporated into cellular DNA. Clearly, at this level of hydroxyurea, some DNA breaks down during the first 60 min of the block and a low level of resynthesis occurs. However, when excess unlabeled thymidine is added along with the hydroxyurea to the cultures, it is unlikely that significant amounts of [<sup>3</sup>H]thymidine are incorporated into DNA under the "chase" conditions.

**"Pulse-Chase" experiments with infected cultures.** Synchronized RT-7 cells were infected and exposed to [<sup>3</sup>H]thymidine (150  $\mu$ Ci/ml) for 2 h, beginning 28 h after mitotic detachment. After 2 h, the medium was removed, the cultures were rinsed, and medium containing hydroxyurea and unlabeled thymidine was added as described above. Samples were taken at intervals after the addition of [<sup>3</sup>H]thymidine and after "chase" conditions were instituted. The full virus material (110S) was isolated from each sample on sucrose gradients. Throughout the experiment, the total incorporation of

[ $^3\text{H}$ ]thymidine into the cultures was also followed, and the amount of labeled virus released into the culture medium was determined.

As shown in Fig. 13, [ $^3\text{H}$ ]thymidine was incorporated into the cultures at a linear rate from the time of addition until "chase" conditions began at 120 min. Net incorporation into the infected cultures then ceased abruptly and, as observed previously, the amount of precipitable label in the cultures declined. Prior to the "chase," label was incorporated into 110S viral particles at a rate similar to the rate of incorporation into the whole cultures. However, the rate of appearance of label in viral particles may not be absolutely linear. (Note the differences in the two scales in Fig. 13.) Net incorporation of [ $^3\text{H}$ ]thymidine into the full virus particles stopped immediately upon addition of hydroxyurea and unlabeled thymidine. There was no significant decrease in the total amount of label in viral particles (cellular virus plus virus in the medium) during the 120 min of the "chase" period.

The 110S labeled MVM from each cell sample was run on CsCl density gradients and the results are shown in Fig. 14 (note changes in scale). At the end of a 30-min labeling period, over 96% of the [ $^3\text{H}$ ]thymidine in full virus particles was found at the density of 1.46 g/cm<sup>3</sup>.

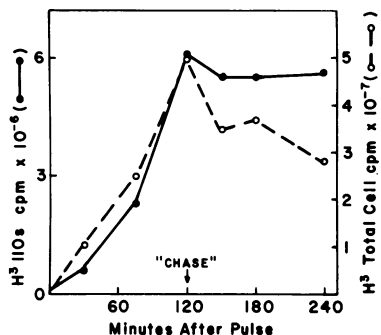


FIG. 13. Incorporation of [ $^3\text{H}$ ]thymidine into cells and into 110S virus before and after addition of hydroxyurea and unlabeled thymidine. Mitotically detached RT-7 cells were infected 3 h after detachment, and 25 h later they were labeled with [ $^3\text{H}$ ]thymidine (150  $\mu\text{Ci}/\text{ml}$ ). After 2 h, the medium was removed, and hydroxyurea (25  $\mu\text{g}/\text{ml}$ ) and unlabeled thymidine (2.5 mM) were added in fresh medium. Total cellular [ $^3\text{H}$ ]thymidine incorporation was determined on a sample of the infected cultures after sonic treatment (○). The total amount of label in 110S virus was determined by trichloroacetic acid precipitation across sucrose gradients run both on tissue culture fluid and on virus extracted from the cultures (as described in Materials and Methods) at each time point (●). At 240 min, 11% of the total viral 110S label was found in the medium.

However, even in this brief interval, detectable amounts of 1.42 material were observed. By 120 min, 72% of the labeled virus was of the 1.46 g/cm<sup>3</sup> class and 28% of the viral label was found at 1.42 g/cm<sup>3</sup>. After 120 min under "chase" conditions, only 26% of the virus-associated label was found at 1.46 g/cm<sup>3</sup> and 74% was present in the 1.42 g/cm<sup>3</sup> particle. These results are summarized in Fig. 15. In these experiments, we have shown that [ $^3\text{H}$ ]thymidine incorporation into DNA stops abruptly upon addition of hydroxyurea and unlabeled thymidine to the cultures. We have also shown that net [ $^3\text{H}$ ]thymidine incorporation into 110S virus stops at the same time. Label was lost from the 1.46 g/cm<sup>3</sup> particle after the "chase" began, but the accumulation of the 1.42 particle continued at an undiminished rate. The total amount of label lost from the 1.46 g/cm<sup>3</sup> particle was comparable to the total amount of label gained by the 1.42 g/cm<sup>3</sup> particle. In addition, the rate of loss of label from the 1.46 g/cm<sup>3</sup> virus approximated the rate of label accumulation by the 1.42 g/cm<sup>3</sup> virus. The simplest explanation for these observations is that the 1.46 g/cm<sup>3</sup> particles are a direct precursor of the 1.42 g/cm<sup>3</sup> particles.

**Virus released to the medium.** During the course of these experiments, about 11% of the total 110S labeled virus was found in the culture medium. In conjunction with cell samples, the culture fluid was analyzed on sucrose gradients. The amount of virus released into the medium was determined by quantitating the amount of [ $^3\text{H}$ ]thymidine label in the 110S region of these gradients. The 110S material isolated from the culture fluid of the 240-min sample was analyzed on a CsCl density gradient: 27% of the [ $^3\text{H}$ ]thymidine label was 1.46 g/cm<sup>3</sup> density and 73% was 1.42 g/cm<sup>3</sup> density. Thus, both density classes of full virus, as well as empty capsids, were found free in the medium. These results are consistent with the idea that disintegration of the infected cells, as observed in electron micrographs, is the primary mechanism of virus release.

**Cellular site of viral processing.** As described above, we have noted the persistence of 1.46 g/cm<sup>3</sup> particles in viral preparations isolated late in the course of infection of unsynchronized cultures. It appeared that a small proportion of virus particles was never converted to the 1.42 g/cm<sup>3</sup> particle. In the following experiment, we attempted to explain the persistence of unprocessed particles by determining whether viral processing is restricted to a particular cellular site. RT-7 cells were synchronized and infected as before. The cultures were exposed to [ $^3\text{H}$ ]thymidine (150  $\mu\text{Ci}/\text{ml}$ ) for

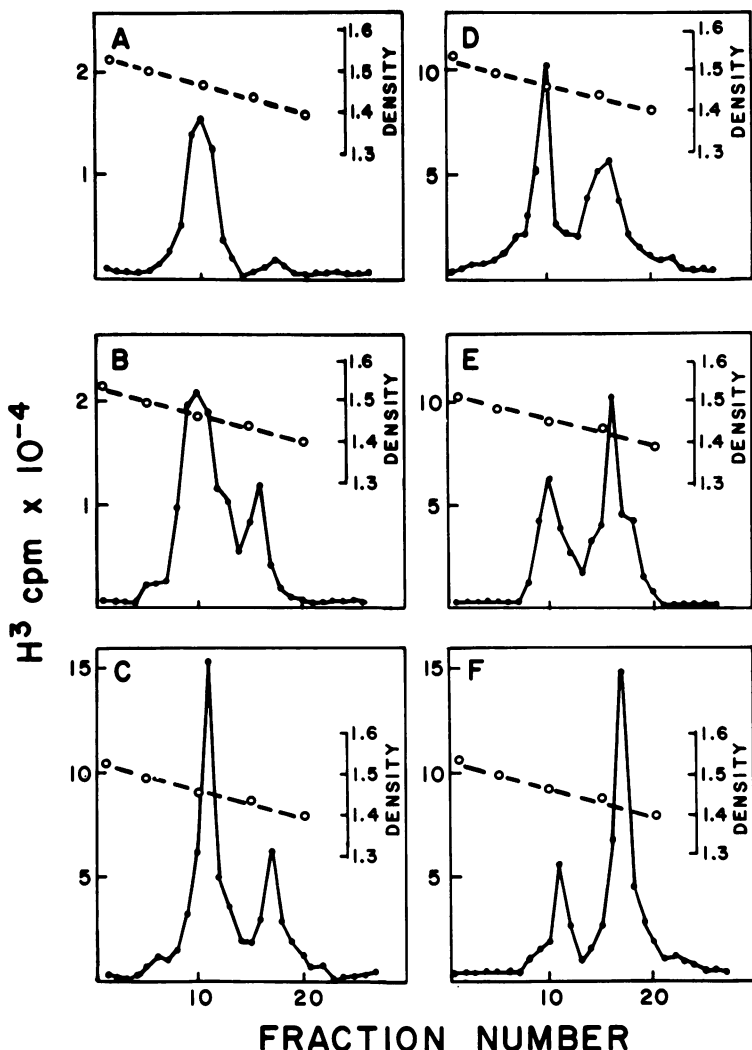


FIG. 14. CsCl gradients of full minute virus of mice isolated from infected synchronized RT-7 cells. The full virus isolated from sucrose gradients in the experiment described in the legend to Fig. 13 was centrifuged to equilibrium in CsCl. Lambda phage was used as a density marker, and the viral peaks were confirmed by hemagglutinin titer. Times: (A) 30 min; (B) 75 min; (C) 120 min; (D) 150 min; (E) 180 min; (F) 240 min.

6 h, beginning at 26 h after mitotic detachment. The medium was then removed, and the cultures were exposed to "chase" conditions for 7 h. Samples were taken at the end of the 6-h labeling period and at the end of the 7-h "chase." For each sample, the cytoplasm and nuclear fractions were separated as described in Materials and Methods. Full virus was isolated from the nuclear and cytoplasmic fractions of each sample by sucrose gradient centrifugation. The 110S viral peak was then analyzed on CsCl density gradients. Labeled 110S virus was found in both the nucleus and the cytoplasm at the end of the 6-h pulse, but by the end of the 7-

h chase most of the [<sup>3</sup>H]thymidine-labeled virus had left the nucleus and the labeled virus in the cytoplasm had increased by 77% (Table 1). Only 60% of the total 110S 6-h label was left in the cell after a 7-h chase. During the "chase" interval, the amount of label in the cell-associated virus particles declined about 40% as a result of excretion of viral particles into the medium.

Table 2 shows the results of the CsCl centrifugation of the 110S virus isolated from the nuclear and cytoplasmic fractions in this experiment. The proportion of 1.46 g/cm<sup>3</sup> particles in the nucleus dropped from 28% of the total at the end of the 6-h labeling period to 11% of the total

at the end of the 7-h chase. In the cytoplasm the relative proportion of  $1.46 \text{ g/cm}^3$  particles to  $1.42 \text{ g/cm}^3$  particles remained essentially the same. In this experiment, the labeling period extended past the point of the peak rate of virus assembly and included a portion of the period when the rate of virus assembly had begun to decline substantially. The relatively high proportion of  $1.42 \text{ g/cm}^3$  particles was probably due to processing of the  $1.46 \text{ g/cm}^3$  particles during this latter period of the labeling interval.

From these data we conclude that the processing of particles of the  $1.46 \text{ g/cm}^3$  density class occurs rapidly in the nucleus. Particles are transported after assembly to the cytoplasm, and this transport appears to occur regardless of whether or not the particles have been processed. Once the  $1.46 \text{ g/cm}^3$  particles have reached the cytoplasm, processing does not occur or occurs at a much reduced rate.

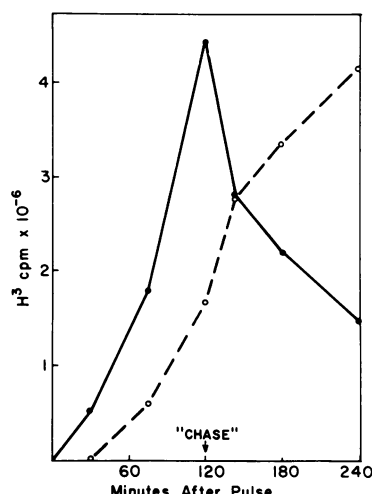


FIG. 15. Kinetics of processing of  $1.46 \text{ g/cm}^3$  and accumulation of  $1.42 \text{ g/cm}^3$  MVM. The total radioactivity of the infected cultures for each density species of full virus was determined from Fig. 14 and is summarized in this figure. Symbols: ●, particles of  $1.46 \text{ g/cm}^3$  density; ○, particles of  $1.42 \text{ g/cm}^3$  density.

## DISCUSSION

It has been previously shown that synthesis of MVM appears to require some function of the host-cell S phase (13). We have shown that assembly of the viral particles occurs abruptly some 8 h after the end of the S phase. Thus, virus assembly and processing do not appear to be specifically coupled to the host-cell S phase.

We have presented evidence that the  $1.46 \text{ g/cm}^3$  density class of MVM particles are processed to form virus of  $1.42 \text{ g/cm}^3$  density. Processing of the  $1.46 \text{ g/cm}^3$  virus is observed at the time of maximal virus assembly in synchronized cells. Detectable amounts of the processed  $1.42 \text{ g/cm}^3$  virus are formed within 30 min. The processing event occurs most rapidly in the infected cell nucleus, the site of virus assembly. On the basis of these results, we conclude that the conversion of  $1.46 \text{ g/cm}^3$  particles to  $1.42 \text{ g/cm}^3$  particles is an integral step in the events of viral assembly.

MVM is a simple virus structurally, and its assembly and maturation might well be accomplished in a few straightforward steps. However, we have noticed that newly assembled viral particles have a broader band width in CsCl gradients than might be anticipated for a single-density species. It is possible that the  $1.42$  density and the  $1.46$  density classes include a spectrum of particles, which could considerably complicate analysis of viral maturation.

TABLE 1. Compartmentalization of newly synthesized full MVM from infected synchronized RT-7 cells<sup>a</sup>

Time (h) after label- ing	Nuclear $^{3}\text{H}$ -labeled MVM	Cytoplasmic $^{3}\text{H}$ -la- beled MVM
6	99,400 (73%)	36,300 (27%)
13	17,300 (21%)	64,300 (79%)

<sup>a</sup> Cells were synchronized and infected as described in Materials and Methods. At 26 h after mitotic detachment, the cells were labeled, and label was "chased" as described in the text. The separation of nuclear and cytoplasmic fractions and determination of [ $^{3}\text{H}$ ]thymidine in 110S virus is described in Materials and Methods.

TABLE 2. Distribution of newly synthesized  $1.46$  and  $1.42 \text{ g/cm}^3$  MVM in the nucleus and cytoplasm of infected synchronized RT-7 cells<sup>a</sup>

Time (h) after pulse	Nuclear $^{3}\text{H}$ -labeled MVM		Cytoplasmic $^{3}\text{H}$ -labeled MVM	
	$1.46 \text{ g/cm}^3$	$1.42 \text{ g/cm}^3$	$1.46 \text{ g/cm}^3$	$1.42 \text{ g/cm}^3$
6	27,900 (28%)	72,000 (72%)	12,000 (36%)	21,600 (64%)
13	1,200 (11%)	15,400 (89%)	26,000 (41%)	37,200 (59%)

<sup>a</sup> [ $^{3}\text{H}$ ]thymidine-labeled MVM isolated from synchronized RT-7 cells (see footnote, Table 1) was centrifuged to equilibrium in CsCl.

On the other hand, we have not observed any major viral species with densities intermediate between 1.46 and 1.42, nor has there been a gradual shifting of the viral density from 1.46 to 1.42 g/cm<sup>3</sup> during the "chase" experiments.

In a model recently proposed by Tattersall et al. (15), mature single-stranded viral DNA could either be stripped from its template by the process of encapsulation or driven off the template by new DNA synthesis. Some aspects of our results are consistent with the latter form of the Tattersall proposal. In this variation of the model, during a brief exposure to [<sup>3</sup>H]thymidine, old, unlabeled DNA strands would be encapsulated prior to the appearance of labeled DNA in particles. In addition, since DNA synthesis drives encapsulation, inhibition of DNA synthesis would stop new virus assembly even though a large pool of assembly intermediates might be present in the infected cells. (Such subviral assembly intermediates appear to be present in LuIII-infected cells [10].) From our experiments it is not possible to determine whether there is a significant lag between incorporation of [<sup>3</sup>H]thymidine into DNA and appearance of this label in viral particles, although there appears to be a slight difference between these two curves (Fig. 13). However, it is clear that, when DNA synthesis is inhibited, the assembly of virus stops at once.

The role of the empty viral capsid in the viral assembly sequence has not been defined. The empty capsids could be (i) a precursor to the 1.46 g/cm<sup>3</sup> virus by insertion of viral DNA, (ii) a degradation product of the 1.46 g/cm<sup>3</sup> virus through extrusion of viral DNA, or (iii) an independently assembled particle unrelated to full virus. The empty capsids are detected slightly prior to the appearance of full virus both in electron micrographs and in extracts of synchronized infected cultures. On this basis and because we have shown a quantitative transfer of [<sup>3</sup>H]thymidine label from the 1.46 g/cm<sup>3</sup> to the 1.42 g/cm<sup>3</sup> class, it seems unlikely that the empty capsids are produced by loss of DNA from the 1.46 density particles.

It is possible that the empty capsids are precursors to the 1.46 g/cm<sup>3</sup> virus. However, assembly of the 1.46 g/cm<sup>3</sup> particles is immediately halted when DNA synthesis is inhibited. As there are large amounts of empty capsids present in the infected cell, either the pool of single-stranded viral DNA available for insertion must be very small, or insertion requires ongoing DNA synthesis, perhaps as a driving force for this process.

Regardless of the actual relationship between the empty capsids and the 1.46 g/cm<sup>3</sup> virus particle, it is clear that the presence of

viral DNA has a profound effect on the surface properties of the particle. The empty capsid and the 1.46 g/cm<sup>3</sup> virus contain the same proteins in the same proportions; yet the 1.46 g/cm<sup>3</sup> particle hemagglutinates mouse red blood cells poorly and is readily processed to the 1.42 g/cm<sup>3</sup> form by proteolytic cleavage. On the other hand, the empty capsid particles have a high hemagglutination activity but are very resistant to proteolytic processing both *in vivo* and *in vitro* (3, 14).

In the sequence of MVM assembly, virus is first detected in the nucleus and appears shortly afterwards in the cytoplasm and in the culture medium. All three classes of virus particles move out of the nucleus to the cytoplasm and into the medium with equal facility. In electron micrographs we have found no evidence of any virus-specific transport process, either from the nucleus to the cytoplasm or out of the cell. It appears likely that virus particles are expelled from the nucleus by some generalized process such as margination of chromatin and blistering of the nuclear membrane. Similarly, virus particles spill into the medium, probably during cellular disintegration. Membrane fragments coated with virus particles are a common feature of cultures in the last stages of infection.

The processing of viral particles after their assembly is by no means unique to MVM. For example, the capsid proteins of poliovirus particles undergo proteolytic cleavage during maturation (4). As the requirements for self-assembly of capsid proteins are not necessarily those which produce a particle with optimal infectivity, proteolytic "trimming" after virus assembly may represent an economical means of satisfying two disparate demands of virus formation.

#### ACKNOWLEDGMENTS

We gratefully acknowledge helpful discussions with Peter Tattersall and David Ward during the course of this work. Helen Bruning provided expert technical assistance.

This investigation was supported by Public Health Service grants 1 KO4 CA 00134 and 5 RO1 CA 16517 from the National Cancer Institute, by grant 1-396 from the National Foundation-March of Dimes, and by a grant from the United Fund Health Foundation of Canton, Ohio.

#### LITERATURE CITED

1. Bachman, P. A., M. D. Hoggan, J. L. Melnick, H. G. Percira, and C. Vago. 1975. Parvoviridae. *Intervirology* 5:85-92.
2. Clinton, G. M., and M. Hayashi. 1975. The parvovirus MVM: particles with altered structural proteins. *Virology* 66:261-267.
3. Clinton, G. M., and M. Hayashi. 1976. The parvovirus MVM: a comparison of heavy and light particle infectivity and their density conversion *in vitro*. *Virology* 74:57-63.
4. Fernandez-Tomas, C. G., and D. Baltimore. 1973. Morphogenesis of poliovirus. II. Demonstration of a new

- intermediate, the proviron. *J. Virol.* 12:1122-1130.
- 5. **Hampton, E. G.** 1970. H-1 virus growth in synchronized rat embryo cells. *Can. J. Microbiol.* 16:266-268.
  - 6. **Laemmli, U.** 1970. Cleavage of structural proteins during the assembly of the head of bacteriophage T4. *Nature (London)* 227:680-685.
  - 7. **Reynolds, E. S.** 1963. The use of lead citrate at high pH as an electron opaque stain in electron microscopy. *J. Cell Biol.* 17:208-219.
  - 8. **Rose, J. A.** 1974. Parvovirus reproduction, p. 1-61. In *H. Fraenkel-Conrat and R. R. Wagner (ed.), Comprehensive virology*, vol 3. Plenum Press, New York.
  - 9. **Siegl, G., and M. Gautschi.** 1973. The multiplication of parvovirus LuIII in a synchronized culture system. I. Optimum conditions for virus replication. *Arch. Gesamte Virusforsch.* 40:105-118.
  - 10. **Siegl, G., and M. Gautschi.** 1976. Multiplication of parvovirus LuIII in a synchronized culture system. III. Replication of viral DNA. *J. Virol.* 17:841-853.
  - 11. **Singer, I. I.** 1975. Ultrastructural studies of H-1 parvo-virus replication. II. Induced changes in the deoxyribonucleoprotein and ribonucleoprotein components of human NB cell nuclei. *Exp. Cell Res.* 95:205-217.
  - 12. **Singer, I. I., and H. W. Toolan.** 1975. Ultrastructural studies of H-1 parvovirus replication. I. Cytopathology produced in human NB epithelial cells and hamster embryo fibroblasts. *Virology* 65:40-54.
  - 13. **Tattersall, P.** 1972. Replication of the parvovirus MVM. I. Dependence of virus multiplication and plaque formation on cell growth. *J. Virol.* 10:586-590.
  - 14. **Tattersall, P., P. J. Cawte, A. J. Shatkin, and D. C. Ward.** 1976. Three structural polypeptides coded for by minute virus of mice, a parvovirus. *J. Virol.* 20:273-289.
  - 15. **Tattersall, P., and D. C. Ward.** 1976. Rolling hairpin model for replication of parvovirus and linear chromosomal DNA. *Nature (London)* 263:106-109.
  - 16. **Wray, W.** 1975. Parallel isolation procedures for metaphase chromosomes, mitotic apparatus, and nuclei. *Methods Enzymol.* 40:75-89.